Cembranoid and Long-Chain Alkanol Sites on the Nicotinic Acetylcholine Receptor and Their Allosteric Interaction†

Oné R. Pagán,‡,§ Vesna A. Eterović,‡ Miosotis Garcia,‡ Derick Vergne,‡ Carlos M. Basilio,|| Abimael D. Rodríguez,⊥ and Richard M. Hann*,‡

Department of Biochemistry and Center for Molecular and Behavioral Neuroscience, Universidad Central del Caribe, Bayamón, Puerto Rico, Department of Biochemistry, University of Puerto Rico, Medical Sciences Campus, San Juan, Puerto Rico, and Department of Chemistry, University of Puerto Rico, Río Piedras Campus, San Juan, Puerto Rico

Received June 13, 2001

ABSTRACT: Long-chain alkanols are general anesthetics which can also act as uncharged noncompetitive inhibitors of the peripheral nicotinic acetylcholine receptor (AChR) by binding to one or more specific sites on the AChR. Cembranoids are naturally occurring, uncharged noncompetitive inhibitors of peripheral and neuronal AChRs, which have no demonstrable general anesthetic activity in vivo. In this study, [^{3}H]-tenocyclidine ([^{3}H]TCP), an analogue of the cationic noncompetitive inhibitor phencyclidine (PCP), was used to characterize the cembranoid and long-chain alkanol sites on the desensitized *Torpedo californica* AChR and to investigate if these sites interact. These studies confirm that there is a single cembranoid site which sterically overlaps the [^{3}H]TCP channel site. This cembranoid site probably also overlaps the sites for the cationic noncompetitive inhibitors, procaine and quinacrine. Evidence is also presented for one or more allosteric cembranoid sites which negatively modulate cembranoid affinity for the inhibitory site. In contrast, long-chain alkanols inhibit [^{3}H]TCP binding through an allosteric mechanism involving two or more alkanol sites which display positive cooperativity toward each other. Double inhibitor studies show that the cembranoid inhibitory site and the alkanol sites are not independent of each other but interfere allosterically with each other's inhibition of [^{3}H]TCP binding. The simplest models consistent with the observed data are presented and discussed.

The peripheral nicotinic acetylcholine receptor (AChR)[1] found in the postsynaptic membranes of muscle and electric organs is a ligand-gated cation channel which has been an important model for studying how general anesthetics interact with membrane proteins (*1*). The peripheral AChR is probably not an anesthetic target in vivo, but homologous ligand-gated ion channels, such as neuronal AChRs and the γ-aminobutyric acid and glycine receptors, may be targets of such compounds (*2*, *3*). The AChR is a pentameric transmembrane protein with subunit stoichiometry of $\alpha_2\beta\gamma\delta$ whose channel is located in the axis of pseudosymmetry formed by the five homologous subunits, each of which has four transmembrane segments, M1−M4 (*4*−*6*). The walls of the channel are formed mainly by α-helical M2 segments from all five subunits (*7*, *8*), but the nonhelical M1 segments probably also contribute to the channel walls (*9*, *10*). The amino acid sequences of the five M2 helices give the channel a stratified structure such that residues at homologous positions facing the lumen form rings with distinct properties which determine channel parameters (*11*). This stratification includes rings of polar residues in the lower half of the channel and a stack of two or three rings which create a hydrophobic domain in the upper half of the channel. A second hydrophobic AChR domain exists at the membrane lipid−receptor interface, which is formed mainly by the M3 and M4 transmembrane segments (*12*, *13*).

Noncompetitive inhibitors (NCIs) of the AChR block agonist-induced ion flow through the channel by binding to sites different from the two agonist-binding sites. They are a structurally heterogeneous group of compounds which includes cationic molecules, such as local anesthetics and the hallucinogen, PCP, as well as uncharged molecules, such as steroids (*14*), cembranoids (*15*), the lipophilic photoreactive reagent, TID (*16*), and certain general anesthetics, including long-chain alkanols (*17*, *18*). The only structural feature which all NCIs share is a significant degree of hydrophobicity.

The binding sites of uncharged NCIs are not as well characterized as those of the cationic NCIs, which bind in a voltage-dependent manner to one high-affinity site per *Torpedo* AChR molecule (reviewed in ref *19*). In most proven cases, this site is located within the channel domain

† Supported by Grants NIH-NCRR-RCMI-SNRP-U54-NS39408 and NIH-MBRS-SO6GM50695 (to R.M.H.) and NIH-RO1-GM52227 and NIH-RCMI-2G12RR03035 (to V.A.E.). O.R.P. was a recipient of a Viets Fellowship from the Myasthenia Gravis Foundation of America.

* To whom correspondence should be addressed: Department of Biochemistry and Center for Molecular and Behavioral Neuroscience, Universidad Central del Caribe, Box 60-327, Bayamón, PR 00960. Telephone and fax: (787) 786-6285. E-mail: hannbio@coqui.net.

‡ Universidad Central del Caribe.

§ Present address: Department of Molecular Medicine, Veterinary Medical Center, Cornell University, Ithaca, NY 14853.

|| Department of Biochemistry, University of Puerto Rico.

⊥ Department of Chemistry, University of Puerto Rico.

[1] Abbreviations: AChR, nicotinic acetylcholine receptor; NCI, noncompetitive inhibitor; CCh, carbamoylcholine; PCP (phencyclidine), 1-(1-phenylcyclohexyl)piperidine; TCP (tenocyclidine), 1-(1-thienylcyclohexyl)piperidine; DMSO, dimethyl sulfoxide; Bgt, α-bungarotoxin.

10.1021/bi0112255 CCC: $20.00
Published on Web 08/23/2001

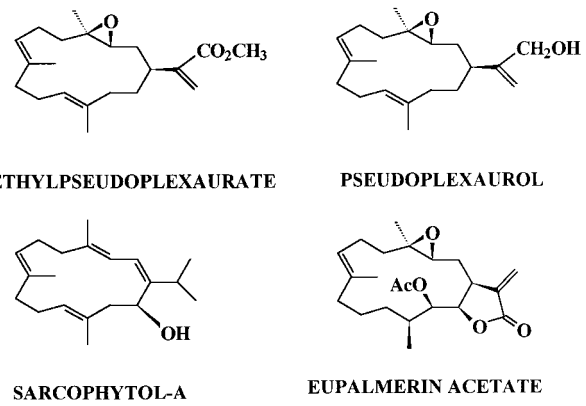

FIGURE 1: Structures of the four cembranoids used in this study.

formed by the M2 helices. However, cationic NCIs can also bind to multiple low-affinity sites which are probably located at the lipid−receptor interface (*20*). It is not certain if cationic NCIs physically plug the channel, as originally proposed (*21*), or interfere allosterically with channel opening (*22*).

Long-chain alkanols inhibit the AChR noncompetitively via one or more sites on the AChR which are distinct from the sites through which short-chain alkanols potentiate AChR ion flux (*23*, *24*). The ability of long-chain alkanols to inhibit both radiolabeled NCI binding to the desensitized *Torpedo* AChR and ion flux through the functional *Torpedo* AChR is directly proportional to the number of carbons in the chain (*24*, *25*). In the case of ion flux, this proportionality extends only up to 12 carbons, above which there is a sharp drop in inhibitory potency. The potency of a homologous group of uncharged general anesthetics, the cycloalkanemethanols, in inhibiting ion flux is also proportional to the number of carbons, with a cutoff seen at 10 carbons (*26*). *n*-Heptanol and *n*-octanol weaken each other's ability to inhibit *Torpedo* AChR ion flux in a manner that suggests that these two alkanols compete for a single inhibitory site (*27*). These observations support the proposal of a single hydrophobic alkanol site on the functional *Torpedo* AChR which does not accommodate molecules larger than 320−340 Å^3. Studies with the embryonic mouse muscle AChR concluded that alkanols inhibit ion flow by binding to a hydrophobic patch in the middle of the M2 channel domain which is large enough to accommodate only one long-chain alkanol molecule at a time (*28*, *29*). When incubated with the desensitized *Torpedo* AChR, the photolabile 3-azirinyl-*n*-octanol labels mainly the glutamate residues at position 20′ of the two α-subunit M2 segments, near the top of the M2 channel domain (*30*). This labeling is saturable and blocked by the cationic NCI, meproadifen, whose photolabile derivative labels the same residue, indicating that long-chain alkanols probably also bind in the M2 channel domain of the desensitized *Torpedo* AChR.

Cembranoids are naturally occurring diterpenoids which contain a 14-member cembrane ring (Figure 1). Cembranoids are found in relatively large amounts in marine gorgonians and soft corals, where they can account for as much as 2−3% of the tissue dry weight (*31*). Their biological role has not been clearly established, but it is generally believed that they deter predation by reef carnivores and help the organism compete for space in the crowded reef environment (*32*). Marine cembranoids are released into the surrounding seawater where they can reach micromolar concentrations (*33*). At these levels, a number of cembranoids have been shown to be ichthyotoxic (*34*). Cembranoids are also found in the cuticle wax of the leaves and flowers of the tobacco plant (*34*). Their biological role in this organism has not been demonstrated, but is probably to defend against herbivore predation.

It is not known how cembranoids achieve their biological effects at the molecular level. Pharmacologically, cembranoids have been shown to inhibit specific enzymes in several different pathways, including carbohydrate metabolism, prostaglandin synthesis, and protein prenylation. This lab first reported that cembranoids in the low micromolar range reversibly and noncompetitively inhibit the AChR of electric organ and mouse muscle (*15*). Cembranoids similarly inhibit the α3β2 and α4β2 rat neuronal AChRs and the α3β4 and α4β2 human neuronal AChRs (*35*). This effect on central AChRs may be related to the recently observed blockage by tobacco cembranoids of nicotine-induced behavioral sensitization in rats (*35*).

The cembranoids include lophotoxin and its analogues which act as irreversible, competitive inhibitors of the AChR by binding covalently at the agonist sites (*36*). However, most cembranoids that have been studied do not bind with measurable affinity at the agonist sites (*15*, *37*). In line with this, cembranoids inhibit [^{3}H]PCP binding to its high-affinity channel site on the desensitized *Torpedo* AChR in a mutually exclusive manner either by competing sterically for the same site or via a strong allosteric effect (*37*). Even lophotoxin shows this effect, although at much lower potency than its competitive effect. Studies on a series of cembranoids indicated that the hydrophobicity of the cembranoid molecule, especially between carbons 7 and 14, was an important determinant of its affinity for the AChR (*37*).

As the target of many biological toxins, the AChR could also be the main target for the marine and tobacco cembranoids, which has important pharmacological and clinical implications. For this reason, it is essential to understand how these diterpenes interact with the AChR. These studies were undertaken to further characterize the cembranoid and long-chain alkanol binding sites on the desensitized *Torpedo* AChR and the relationship of these sites to each other. Since [^{3}H]PCP is no longer commercially available, a PCP analogue, [^{3}H]TCP, was employed as a channel probe of the AChR. Some of the data in this paper were previously published in thesis form (*38*).

EXPERIMENTAL PROCEDURES

Materials. Torpedo californica electric organ was obtained frozen (Pacific Biomarine, Venice, CA). [^{3}H]TCP (41−50 Ci/mmol) and [^{125}I]-Tyr54-α-bungarotoxin (Bgt) (104−128 Ci/mmol) were from DuPont-New England Nuclear (Boston, MA). The cembranoids that were studied were natural products extracted from marine coelenterates whose purification and characterization have been described previously (*37*). Sarcophytol-A was a kind gift from M. Kobayashi (Hokkaido University, Hokkaido, Japan).

Preparation and Characterization of AChR-Rich Membranes. AChR-rich membranes were prepared from the total membrane fraction of homogenized *T. californica* electric organ as previously described (*39*). The amount of total membrane protein was determined by the Lowry method (*40*)

using bovine serum albumin as a standard. The AChR was quantified as the total number of [^{125}I]Bgt binding sites in the solubilized AChR using a filtration assay previously described (*41*), as modified (*39*). The specific activity of the AChR in membrane preparations ranged from 0.2 to 0.5 nmol of AChR/mg of protein.

Radioligand Binding Assays. [^{3}H]TCP binding to the membrane-bound AChR was assessed using a filtration assay previously described for [^{3}H]PCP binding (*37*). The amount of specifically bound [^{3}H]TCP was calculated by subtracting the amount of nonspecifically bound ligand, measured in samples preincubated with either 1 mM tetracaine or 30 μM unlabeled PCP, from the amount of total bound ligand. Under these conditions, the amount of nonspecifically bound [^{3}H]-TCP was always less than 15% of the total amount bound and was mainly due to binding to the filters as demonstrated by filter blanks in the absence of membranes. The desensitized AChR conformation was maintained by the presence of 100 μM carbamoylcholine (CCh) and low-ionic strength buffer [10 mM sodium phosphate and 5 mM NaEDTA (pH 7.4)] which are known to stabilize it (*42*).

For binding experiments under equilibrium conditions, the final concentrations in the incubation mixtures were 150−200 nM AChR, 100 μM CCh, 5% DMSO, and 250 nM [^{3}H]-TCP. [^{3}H]TCP was diluted with unlabeled TCP to 10% of its initial specific activity. At half-saturating concentrations, [^{3}H]TCP binding to the agonist-desensitized AChR reached equilibrium in ~5 min and was stable for at least 30 min (data not shown). Under these conditions, the level of binding was linear up to ~30% of total [^{3}H]TCP bound. All equilibrium binding experiments were carried out within these time and radioligand concentration ranges. Concentration curves for each inhibitor (I) in the absence or presence of a second inhibitor were initially analyzed by fitting equilibrium binding data from at least three experiments to the following logistic (Hill-type) equation (*27*):

$$[RT]/[RT]_c = \{1/[1 + ([I]/IC_{50})^{n_H}]\}(1 - F) + F \quad (1)$$

where $[RT]_c$ is the level of specific binding in the absence of I (control), [I] is the unbound inhibitor concentration (approximated as the total inhibitor concentration), IC_{50} is the inhibitor concentration producing 50% inhibition of [^{3}H]-TCP binding, n_H is the slope (or Hill) coefficient of the inhibition curve, and F is the fraction of specific binding that is not inhibited by I. For statistical analysis of these parameters, eq 1 was fit to the data from individual experiments, thus producing three or four values for each parameter under each condition. The one-sample Student's t test was used to ascertain if the slope coefficients were significantly different from 1 and if the F values were significantly different from 0. A two-sample, unpaired t test was used to test the difference between the values of one parameter under two different conditions, while one-way ANOVA was used to test the difference between the values of one parameter under three different conditions. A probability (p) value of <0.05 was considered statistically significant.

The [^{3}H]TCP dissociation rate in the presence or absence of inhibitor was determined by first preincubating membranes for 20 min at 25 °C in low-ionic strength buffer [10 mM sodium phosphate and 5 mM EDTA (pH 7.4)] containing CCh and DMSO. Then [^{3}H]TCP was added and the mixture incubated in a rotator for an additional 20 min at 25 °C. Concentrations in the incubation mixture were as follows: 150 nM AChR, 100 μM CCh, 5% DMSO, and 50 nM [^{3}H]-TCP. To the mixture was then added an equal volume of the same buffer (without membranes or [^{3}H]TCP) containing 60 μM unlabeled PCP and either no inhibitor (control) or inhibitor at twice the desired final concentration. At specific times, 100 μL aliquots were filtered through glass fiber filters over vacuum and washed quickly with 1.0 mL of buffer. Dissociation rate data were fit to the exponential equation:

$$[RT]_t = [RT]_o e^{-kt} \quad (2)$$

where $[RT]_t$ and $[RT]_o$ are the concentrations of specifically bound [^{3}H]TCP at time t and time zero, respectively, and k is the observed dissociation rate constant corresponding to an initial complex concentration of $[RT]_o$.

Data analyses were performed using either the PSI-Plot program (Poly Software International, Salt Lake City, UT) or the Mathcad program (Mathsoft, Cambridge, MA). Molecular volumes were calculated by dividing the molar volume determined using the MolSuite 2000 program (ChemSW, Fairfield, CA) by Avogadro's number.

RESULTS

Cembranoid Inhibition of [^{3}H]TCP Binding to the Desensitized AChR. Under equilibrium conditions, the four cembranoids used in this study (Figure 1) completely inhibited [^{3}H]TCP binding to the desensitized AChR (Figure 2). The IC_{50}s were slightly lower than values reported for [^{3}H]PCP binding to equivalent membrane preparations under the same conditions (Table 1), probably due to the slightly higher affinty of [^{3}H]TCP for the desensitized AChR: K_D-(TCP) = 0.25 ± 0.04 μM versus K_D(PCP) = 0.30 ± 0.10 μM (*38*). Fitting data to eq 1 gave slope coefficients for all the cembranoid inhibition curves of <1 due to digression from the single-inhibitory site model at very low cembranoid concentrations, where a plateau was observed. However, when only data in the main part of the inhibition curves were fit to eq 1 were the slope coefficients not different from 1.

Although the complete inhibition seen at high cembranoid concentrations is consistent with steric inhibition, a strong allosteric inhibition cannot be ruled out by the equilibrium binding data. To address this question, the effect of cembranoid on the [^{3}H]TCP dissociation rate was measured. The rate of [^{3}H]TCP dissociation from the desensitized AChR fit closely to an exponential rate equation (eq 2; Figure 3A). The dissociation rate in the presence of methylpseudoplexaurate at 0.5 μM (near its IC_{50}) followed the same exponential function that was observed in the absence of cembranoid. The observed dissociation rate constants (2.03 ± 0.19 and 2.07 ± 0.16 min^{-1}) and initial receptor−ligand complex concentrations (8.2 ± 0.8 and 8.2 ± 0.7 nM) in the absence and presence of cembranoid, respectively, did not differ significantly (mean ± standard deviation from three experiments). These findings demonstrate that cembranoid inhibition of [^{3}H]TCP binding is steric in nature, since allosteric inhibition of ligand binding is nearly always associated with a change in the observed ligand dissociation rate due to the additional involvement of a ternary complex (*43*, *44*). Slope

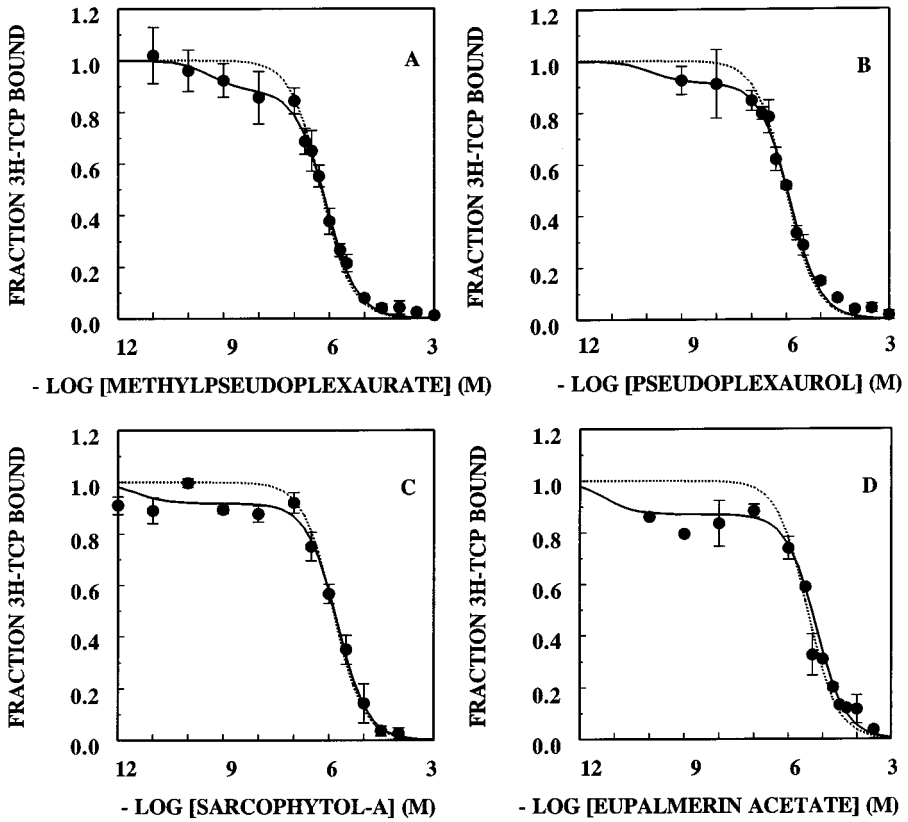

FIGURE 2: Cembranoid inhibition of [^{3}H]TCP binding to the desensitized *Torpedo* AChR under equilibrium conditions. Inhibition of [^{3}H]-TCP binding was assessed as described in the Experimental Procedures. The cembranoids that were studied were (A) methylpseudoplexaurate, (B) pseudoplexaurol, (C) sarcophytol-A, and (D) eupalmerin acetate. Fraction bound represents the level of specific [^{3}H]TCP binding normalized to the level of binding in the absence of cembranoid. Each value shown is the mean ± standard error of the mean (SEM) from three experiments; where error bars are not visible, the SEM was within the range of the symbol. The inhibition curves were generated by computer fitting the data to the model equation for a single steric inhibitory site (eq 1 with $n = 1$ and $F = 0$, dotted line) and to model eq 3 (solid line). Fittings to eq 3 gave the following values for S, S', A, and A' (all nanomolar): 1.8, 350, 0.5, and 98 for methylpseudoplexaurate; 0.8, 448, 0.2, and 112 for pseudoplexaurol; 0.02, 794, 0.004, and 143 for sarcophytol-A; and 0.02, 1680, 0.01, and 840 for eupalmerin acetate, respectively.

Table 1: Parameters of Cembranoid and Long-Chain Alkanol Inhibition of [^{3}H]TCP Binding to the Desensitized *Torpedo* AChR[a]

inhibitor	IC_{50} (μM)	n_H	IC_{50} (μM) vs [^{3}H]PCP[b]
cembranoids			
methylpseudoplexaurate	0.60 ± 0.07	0.79 ± 0.08	0.9 ± 0.1
pseudoplexaurol	1.04 ± 0.11	0.79 ± 0.07	1.2 ± 0.1
sarcophytol-A	0.81 ± 0.13	0.67 ± 0.08	1.7 ± 0.3
eupalmerin acetate	3.14 ± 0.53	0.70 ± 0.08	8.6 ± 0.6
alkanols			
n-hexanol	7079 ± 1449	0.92 ± 0.17	NR[c]
n-heptanol	5343 ± 1113	0.88 ± 0.16	NR[c]
n-octanol	706 ± 49	1.50 ± 0.12	1100 ± 100
n-nonanol	136 ± 11	2.89 ± 0.59	NR[c]
n-decanol	105 ± 11	1.72 ± 0.27	NR[c]

[a] IC_{50} and the slope coefficient (n_H) were obtained by fitting experimental data to eq 1. Shown are means ± SD from three or four experiments. [b] From ref *37*. [c] Not reported.

coefficients of 1 indicate that this steric inhibition occurs via a single cembranoid site.

Under equilibrium conditions, the cationic NCIs, procaine and quinacrine, at concentrations near or just above their IC_{50}s, displaced the methylpseudoplexaurate inhibition curve to the right without changing the slopes of the curves (Figure 4A, IC_{50}s of 0.53 ± 0.02 μM for control, 0.96 ± 0.04 μM in 212 μM procaine, and 1.58 ± 0.10 μM in 424 μM procaine; Figure 4B, IC_{50}s of 1.25 ± 0.17 μM for control and 2.77 ± 0.41 μM in 1 μM quinacrine). This displacement was overcome by high cembranoid concentrations, indicating that the cembranoid binding and procaine or quinacrine binding are mutually exclusive. The cembranoid IC_{50} increases are close to what is predicted by the simple competitive inhibition model (*27*).

Long-Chain Alkanol Inhibition of [^{3}H]TCP Binding to the Desensitized AChR. The long-chain alkanols (6−10 carbons) all inhibited [^{3}H]TCP binding in a concentration-dependent manner (Figure 5A). The inhibitory potencies (measured as IC_{50}s) were directly proportional to chain length with *n*-decanol being the most potent of those tested (Table 1). This is consistent with an earlier report on *n*-alkanol inhibition of [^{3}H]histrionicotoxin binding to the desensitized *Torpedo ocellata* AChR (25). In the case of the three longest alkanols, inhibition was incomplete at the highest obtainable concentrations. Fitting data to eq 1 gave F values significantly different from zero: 0.12 ± 0.02 ($p < 0.005$) for *n*-octanol, 0.18 ± 0.02 ($p < 0.002$) for *n*-nonanol, and 0.08 ± 0.03 ($p < 0.025$) for *n*-decanol. In the case of *n*-hexanol and *n*-heptanol, the data could not be extended to sufficiently high concentrations to determine the completeness of the inhibition.

Since incomplete inhibition suggests an allosteric mechanism when solubility is not a factor, the rate of [^{3}H]TCP dissociation from the desensitized AChR was measured in

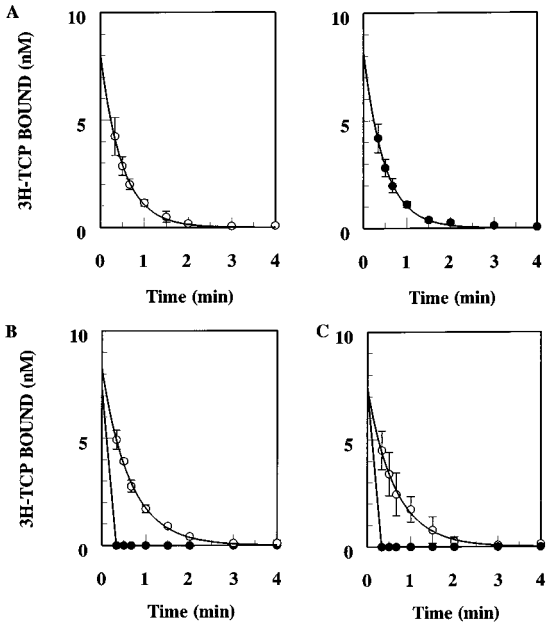

FIGURE 3: Rate of [^{3}H]TCP dissociation from the desensitized *Torpedo* AChR. Membranes were preequilibrated in low-ionic strength buffer with CCh, DMSO, and [^{3}H]TCP as described in Experimental Procedures. Dissociation was initiated by adding an equal volume of the same mixture without [^{3}H]TCP but containing unlabeled PCP and either no inhibitor (○) or inhibitor (●) at twice the desired final concentration. Aliquots were filtered and washed quickly at the indicated times. Inhibitors were (A) methylpseudoplexaurate (1 μM), (B) *n*-octanol (1 mM), and (C) *n*-decanol (300 μM). Each value shown is the mean ± standard deviation (SD) from three experiments. Curves were generated by fitting the data to eq 2.

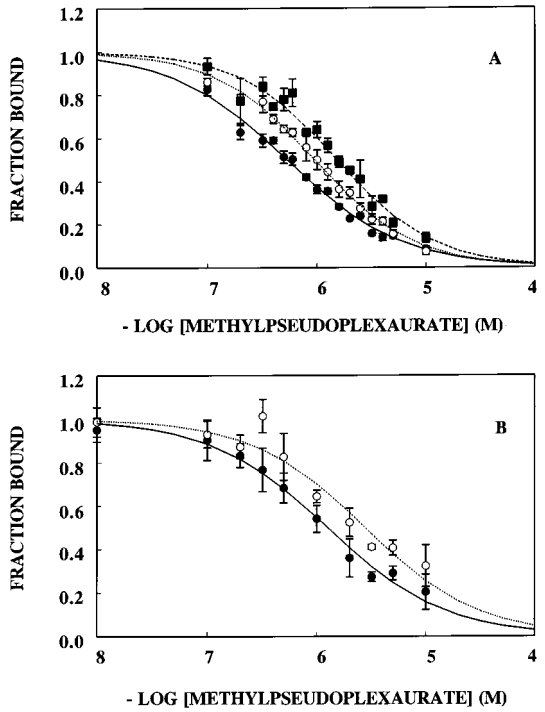

FIGURE 4: Effect of the cationic NCIs, procaine and quinacrine, on methylpseudoplexaurate inhibition of [^{3}H]TCP binding to the desensitized *Torpedo* AChR. Conditions were as described in Experimental Procedures. (A) [^{3}H]TCP binding was assessed in the absence (●, —) or presence of procaine at 212 μM (○, •••) or at 424 μM (■, - - -). (B) [^{3}H]TCP binding was assessed in the absence (●, —) or presence (○, •••) of quinacrine at 1 μM. In both panels, fraction bound represents the level of specific [^{3}H]TCP binding at the indicated cembranoid concentration normalized to control in the absence of cembranoid. Each value shown is the mean ± SEM from three or four experiments. Data were fit to eq 1, and the inhibition curves were generated using the parameters from that fitting, which are given in the text.

the absence and presence of two different alkanols. In the presence of *n*-octanol at a concentration just above its IC_{50}, the rate of [^{3}H]TCP dissociation from the desensitized AChR increased dramatically above that observed in the absence of octanol (Figure 3B). The increase was so great under the conditions that were used that an exponential fitting could not be performed within the minimum sampling time of the experiment (20 s). The same was seen in the presence of *n*-decanol (Figure 3C). This confirms that alkanol inhibition of [^{3}H]TCP binding to the desensitized *Torpedo* AChR involves one or more ternary complexes and is, therefore, allosteric in nature.

The three longest alkanols that were studied gave slope coefficients significantly greater than 1 (Figure 5A and Table 1; $p < 0.025$, $p < 0.01$, and $p < 0.01$ for *n*-octanol, *n*-nonanol, and *n*-decanol, respectively). This suggests that more than one alkanol site is involved in the allosteric inhibition of [^{3}H]TCP binding. At equilibrium, the *n*-octanol inhibition curve was not shifted to the right by the presence of *n*-decanol at a concentration above its IC_{50} (Figure 5B, *n*-octanol IC_{50}s of 706 ± 49 μM for control and 561 ± 121 μM in 200 μM *n*-decanol; $p > 0.05$). Similarly, the *n*-decanol inhibition curve was not shifted significantly by the presence of *n*-octanol at a concentration near its IC_{50} (Figure 5C, *n*-decanol IC_{50}s of 70 ± 5 μM for control and 56 ± 6 μM in 1 mM *n*-octanol; $p > 0.05$). In other words, the apparent affinity of one alkanol for the desensitized AChR was largely unaffected by the presence of the other alkanol, a finding also inconsistent with a single inhibitory site for alkanols. The slope coefficient of the *n*-octanol inhibition curve appeared to decrease from 1.50 ± 0.12 to 1.28 ± 0.30 in the presence of *n*-decanol, and the slope coefficient of the *n*-decanol inhibition curve decreased from 1.82 ± 0.23 to 1.31 ± 0.18 in the presence of *n*-octanol; however, these decreases were not statistically significant ($p > 0.05$). The fraction of [^{3}H]TCP binding not inhibited by *n*-octanol increased significantly from 0.12 ± 0.02 to 0.30 ± 0.05 in the presence of *n*-decanol ($p < 0.02$). The fraction of [^{3}H]-TCP binding not inhibited by *n*-decanol also increased in the presence of *n*-octanol from 0.05 ± 0.02 to 0.11 ± 0.03, but this increase was not statistically significant ($p > 0.05$). Taken together, these findings suggest not only that the allosteric alkanol inhibition of [^{3}H]TCP binding to the desensitized *Torpedo* AChR is mediated via two or more alkanol sites but also that these alkanol sites probably interact with each other in a positive cooperative manner.

The level of procaine inhibition of [^{3}H]TCP binding to the desensitized *Torpedo* AChR was not reduced by the presence of *n*-octanol at concentrations near or above its IC_{50} (Figure 5D). Fitting the data to eq 1 gave IC_{50} values of 377 ± 21 μM for control, 297 ± 54 μM in 1 mM *n*-octanol, and 504 ± 66 μM in 2 mM *n*-octanol. These values do not differ significantly from each other ($p > 0.05$). Therefore, the procaine and octanol sites do not overlap sterically. However, the slope coefficients (0.99 ± 0.05 for control, 0.76 ± 0.12 in 1 mM *n*-octanol, and 1.28 ± 0.20 in 2 mM *n*-octanol) differ significantly from each other ($p < 0.05$). This suggests

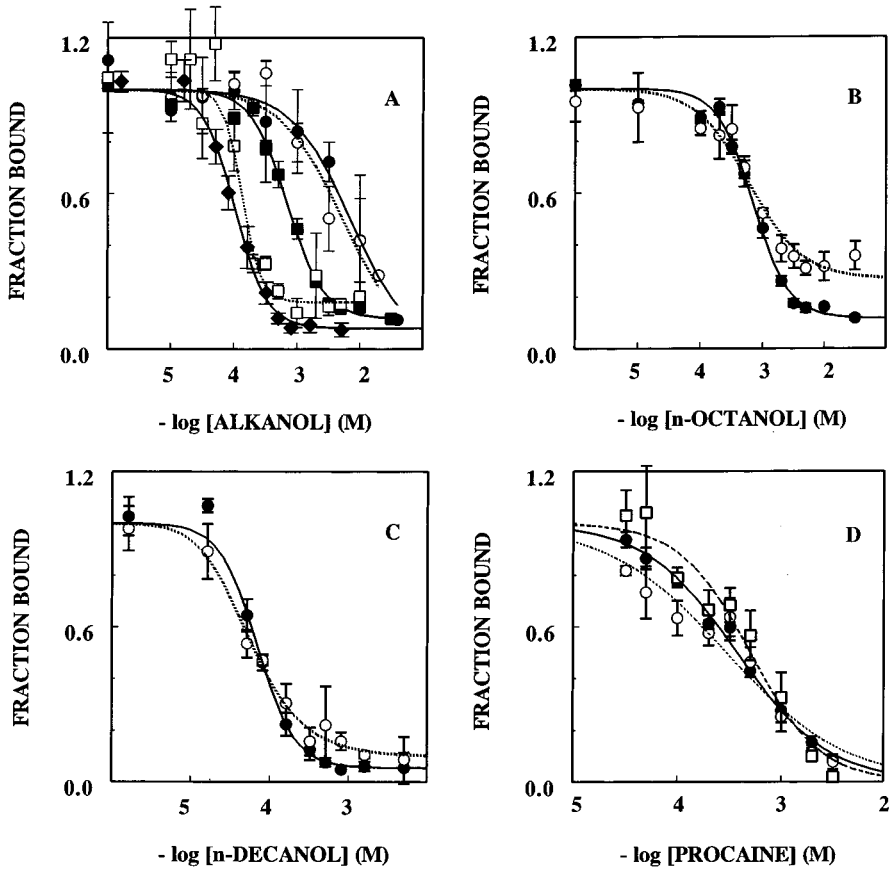

FIGURE 5: Long-chain alkanol inhibition of [^{3}H]TCP binding to the desensitized *Torpedo* AChR under equilibrium conditions. The level of specific [^{3}H]TCP binding to membranes at the indicated concentrations of each alkanol was measured as described in Experimental Procedures. (A) Inhibition of [^{3}H]TCP by *n*-hexanol (●, —), *n*-heptanol (○, ···), *n*-octanol (■, —), *n*-nonanol (□, ···), and *n*-decanol (◆, —). (B) *n*-Octanol inhibition of [^{3}H]TCP binding in the absence (●, —) or presence (○, ···) of 200 μM *n*-decanol. (C) *n*-Decanol inhibition of [^{3}H]TCP binding in the absence (●, —) or presence (○, ···) of 1 mM *n*-octanol. (D) Procaine inhibition of [^{3}H]TCP binding in the absence (●, —) or presence of *n*-octanol at 1 mM (○, ···) or 2 mM (□, - - -). Fraction bound represents the level of specific [^{3}H]TCP binding normalized to the level of binding in the absence of alkanol (A), *n*-octanol (B and D), or *n*-decanol (C). Each value shown is the mean ± SEM from three or four experiments. Data were fit to eq 1, and the parameters from that fitting, which are shown in Table 1 (A) or given in the Results (B−D), were used to generate the curves shown in panels A and D. Data in panels B and C were also fit to model eq 4 ($K = 0.25$ μM) which gave the parameters shown in Table 2. The inhibition curves shown in panels B and C were generated from these parameters.

that some allosteric interaction between the procaine and octanol sites may occur.

Effect of Cembranoids and Long-Chain Alkanols on Each Other's Inhibition of [^{3}H]TCP Binding to the Desensitized AChR. *n*-Octanol was previously reported to decrease the level of methylpseudoplexaurate inhibition of [^{3}H]PCP binding to the desensitized *Torpedo* AChR (*37*). With [^{3}H]-TCP as a radioligand, *n*-octanol, at a concentration above its IC_{50}, appeared to displace the methylpseudoplexaurate inhibition curve to the right (Figure 6A, cembranoid IC_{50}s of 1.02 ± 0.17 μM for control and 5.24 ± 1.31 μM in 2 mM *n*-octanol). However, due to the large error inherent in this type of experiment where more than one-half of the control radioligand binding is inhibited, this change was not statistically significant ($p > 0.05$). The slope was not changed (0.65 ± 0.08 vs 0.59 ± 0.09, $p > 0.05$). *n*-Decanol at a concentration above its IC_{50} significantly decreased the ability of methylpseudoplexaurate to inhibit [^{3}H]TCP binding (Figure 6B, cembranoid IC_{50}s of 0.47 ± 0.04 μM for control and 1.12 ± 0.06 μM in 200 μM *n*-decanol; $p < 0.01$). The presence of *n*-decanol also increased the slope of the cembranoid inhibition curve slightly, but significantly, from 0.89 ± 0.06 to 1.11 ± 0.06 ($p < 0.05$). In contrast, methylpseudoplexaurate, at a concentration near its IC_{50}, did not shift the *n*-decanol inhibition curve significantly (Figure 6C, *n*-decanol IC_{50}s of 160 ± 18 μM for control and 232 ± 97 μM in 1 μM methylpseudoplexaurate; $p > 0.05$) or affect significantly the slope coefficient of the *n*-decanol curve (1.88 ± 0.32 vs 1.47 ± 0.34; $p > 0.05$). However, this cembranoid did increase significantly the fraction of binding not inhibited by *n*-decanol from 0.10 ± 0.04 to 0.29 ± 0.06 ($p < 0.05$). These results show that the cembranoid and alkanol inhibitory sites are not independent of each other, but are inconsistent with simple steric overlap of the cembranoid and alkanol inhibitory sites.

DISCUSSION

PCP/TCP Site. [^{3}H]PCP has often been used as a probe for the cationic NCI site on the desensitized *Torpedo* AChR, since [^{3}H]PCP binds reversibly to this site with a 1:1 stoichiometry and relatively high affinity. The exact location of the PCP site is still not firmly established, since photoaffinity labeling and site-directed mutagenesis studies to date have been inconclusive (*19*). However, much indirect evidence supports a single-channel site for PCP on the

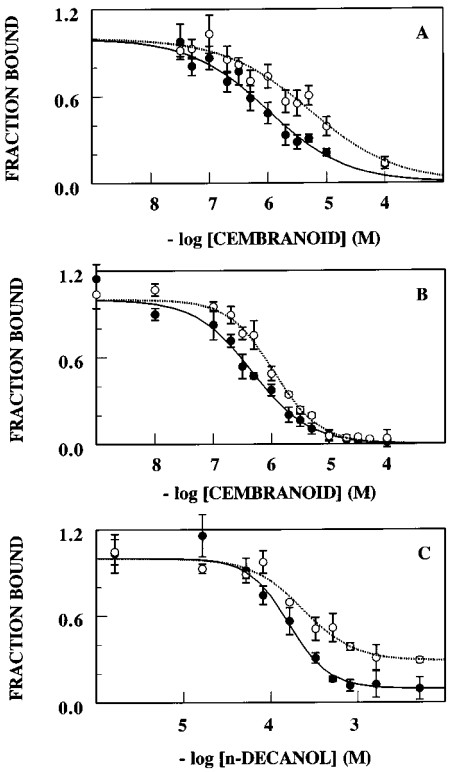

FIGURE 6: Effect of cembranoid and long-chain alkanols on each other's inhibition of [^{3}H]TCP binding to the desensitized *Torpedo* AChR under equilibrium conditions. Methylpseudoplexaurate inhibition of [^{3}H]TCP binding (A) in the absence (●, —) or presence (○, ···) of 2 mM *n*-octanol and (B) in the absence (●, —) or presence (○, ···) of 200 μM *n*-decanol. (C) *n*-Decanol inhibition of [^{3}H]-TCP binding in the absence (●, —) or presence (○, ···) of 1 μM methylpseudoplexaurate. Fraction bound represents the level of specific [^{3}H]TCP binding normalized to control in the absence of cembranoid (A and B) and *n*-decanol (C). Each value shown is the mean ± SD from three or four experiments. Data were fit to eq 1, and the inhibition curves were generated using the parameters from that fitting, which are given in the text.

desensitized *Torpedo* AChR which overlaps the sites for other cationic NCIs (*18*, *20*, *45*−*47*).

Since [^{3}H]PCP is no longer readily available, its commercially available analogue, [^{3}H]TCP, was used in these experiments. Studies in this lab on equivalent membrane preparations have shown that [^{3}H]TCP and [^{3}H]PCP bind to the same site on the desensitized *Torpedo* AChR with similar affinities [K_D(TCP) = 0.25 ± 0.04 μM vs K_D(PCP) = 0.30 ± 0.10 μM] (*38*). Therefore, [^{3}H]TCP can serve as a satisfactory substitute for [^{3}H]PCP as a probe of this site, as was also suggested by recent reports from other labs (*48*, *49*).

Cembranoid Sites. Previous studies on [^{3}H]PCP equilibrium binding to the desensitized *Torpedo* AChR showed that cembranoid and PCP binding are mutually exclusive and that cembranoids compete with each other for inhibition of [^{3}H]-PCP binding (*15*, *37*). These previous findings suggested that cembranoids bind to a single site on the desensitized AChR and compete sterically with PCP for receptor occupancy, but they could not conclusively rule out mutually exclusive binding of cembranoid and PCP through a strong allosteric inhibition mechanism. The observation here, that the presence of cembranoid at half-maximal inhibitory levels does not change the kinetics of [^{3}H]TCP dissociation from the desensitized AChR, is strong evidence that cembranoids compete sterically with TCP (and, by analogy, PCP) for its high-affinity site on the desensitized *Torpedo* AChR. Therefore, the studies presented here confirm that there is one cembranoid inhibitory site on each AChR molecule which sterically overlaps the high-affinity PCP/TCP site.

Both cationic NCIs that were tested, procaine and quinacrine, reduced cembranoid inhibitory potency in a mutually exclusive manner. The degree of cembranoid IC_{50} displacement and the overcoming of this displacement at high cembranoid concentrations are consistent with simple steric competition (*27*). At the concentrations used here, quinacrine and local anesthetics of the procaine class appear to bind in the channel lumen of the desensitized *Torpedo* AChR (*45*, *50*). Therefore, the cembranoid inhibitory site on the densensitized *Torpedo* AChR overlaps these cationic NCI sites and is either in or close to the channel lumen. It has been suggested that many cationic NCIs share a common binding domain with sterically overlapping sites, although nonsteric, charge repulsion effects cannot be ruled out for these positively charged molecules (*45*). The findings here lend further support for the steric occlusion model at a single locus for these NCIs, since significant electrostatic repulsion can be ruled out for the uncharged cembranoid molecule. They also provide further indirect evidence that the N-terminus of the M1 segment, which is photolabeled by quinacrine azide (*9*), forms part of the M2-lined channel domain.

The digression from the single-steric inhibitory site model seen at low cembranoid concentrations (Figure 2) can be accounted for if cembranoids bind with very high affinity to a second allosteric cembranoid site (or set of sites) which decreases cembranoid's affinity for its inhibitory site but is independent of the TCP site (Figure 7A). This model is described by the following equation:

$$f = 1/[1 + (\{[(KC)/(TS)]/(1 + K/T)\}[(1 + C/A')/(1 + C/A)])] \quad (3)$$

where f is the fraction of [^{3}H]TCP bound in the presence of cembranoid versus the absence of cembranoid, T and C are the concentrations of unbound [^{3}H]TCP and cembranoid, respectively, and K, S, A, and A' are equilibrium dissociation constants of the corresponding complexes shown in Figure 7A ($A' > A$). This model fits the cembranoid/[^{3}H]TCP data much better than the single-steric site model and is the simplest model which is consistent with the data. The parameters generated from this fitting (see the legend of Figure 2) suggest that the cembranoid allosteric sites have very high affinity, in the subnanomolar range. Furthermore, the model implies that the initial affinity of cembranoid for its steric inhibitory site is also very high. The putative cembranoid allosteric site(s) may be located in the hydrophobic domain at the lipid−receptor interface, where both cationic and uncharged noncompetitive inhibitors are known to bind (*12*, *19*, *20*).

Long-Chain Alkanol Sites. In contrast to what was seen with cembranoids, alkanol inhibition of [^{3}H]TCP binding to the desensitized *Torpedo* AChR is allosteric in nature and must involve two or more sites which are distinct from the [^{3}H]TCP site. Not surprisingly, the alkanol sites are also sterically distinct from the procaine site, which overlaps the PCP/TCP site. The high slope coefficients together with the substantial fraction of uninhibited TCP binding require that

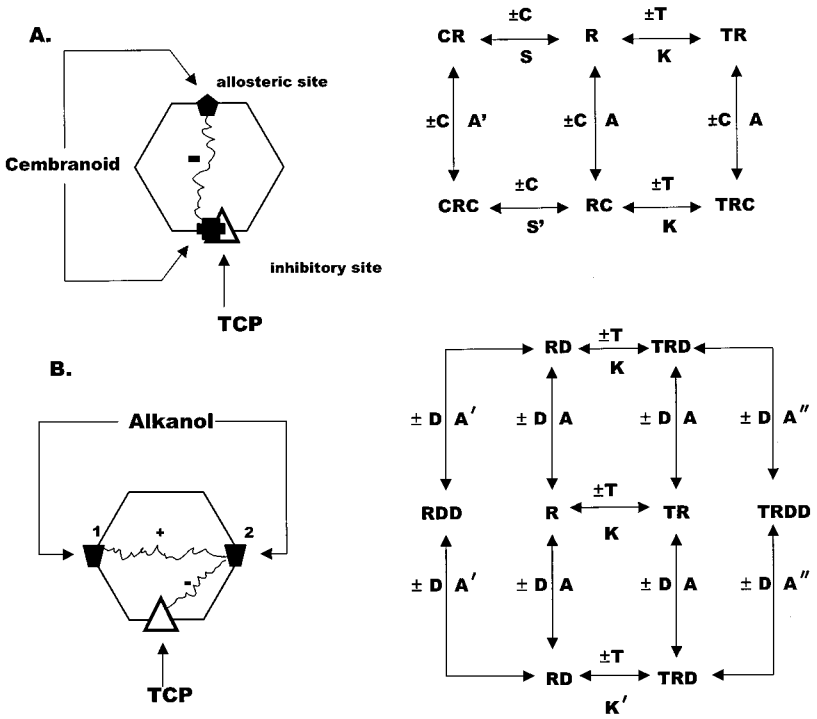

FIGURE 7: Schematic representations of the models for (A) the cembranoid binding sites and (B) the alkanol binding sites. In panel A, R, T, and C are AChR, [^{3}H]TCP, and cembranoid, respectively, and K, S, S', A, and A' are equilbrium dissociation constants of the corresponding complexes ($A' > A$ and $S' > S$). In panel B, D is alkanol and K, K', A, A', and A'' are dissociation constants of the corresponding complexes ($K' > K$ and $A \geq A'' > A'$).

the alkanol sites be linked by positive cooperativity. The simplest model which is consistent with the data contains two alkanol sites which are initially equivalent but display positive cooperativity toward each other and inhibit TCP binding allosterically only when both sites are occupied. This model is shown in Figure 7B and is described by the following equation:

$$f = [1 + (K/T)/(1 + (K/T)\{1 + (2D)/A + [D^2/(AA')]\})]/\{1 + (2D)/A + [D^2/(AA'')]\} \quad (4)$$

where f is the fraction of [^{3}H]TCP bound in the presence of alkanol versus control in the absence of alkanol, T and D are the concentrations of unbound [^{3}H]TCP and alkanol, respectively, and K, A, A', and A'' are equilibrium dissociation constants of the corresponding complexes shown in Figure 7B ($K' > K$ and $A \geq A'' > A'$). The values for these parameters generated by fitting the experimental data graphed in panels B and C of Figure 5 to eq 4 are shown in Table 2. The constant K' is the apparent dissociation constant of [^{3}H]-TCP when both alkanol sites are occupied. The alkanol inhibitory effect (α) can be estimated by the ratio K'/K. The constant A is a measure of the initial alkanol affinity for the AChR, whereas A' is a measure of the affinity of the second alkanol molecule in the absence of TCP. Therefore, the ratio A/A' (β) is an estimate of the positive cooperativity effect of the alkanol.

When the results of the control experiments are compared, the inhibitory effect (α) of decanol alone is only about twice the effect of octanol alone. The initial affinity (A) of decanol is also only about 2 times greater than that of octanol. The much greater potency (lower IC_{50}) as well as the higher slope coefficient of decanol observed (Table 1) are mainly due to decanol's much stronger positive cooperativity effect (β), which is more than 10 times that of octanol.

Table 2: Parameters of *n*-Alkanol Inhibition of [^{3}H]TCP Binding to the *Torpedo* AChR from Model Equation 4[a]

alkanol	K' (μM)	α	A (μM)	A' (μM)	A'' (μM)	β
n-octanol						
control	4.6	19	1455	90	1669	16
with decanol (200 μM)	1.6	6.5	4.4	176	1141	0.03
n-decanol						
control	10.8	43	599	3.4	147	176
with octanol (1 mM)	4.8	19	45	10.5	203	4

[a] Data shown in panels B and C of Figure 5 were fit to eq 4 with K equal to 0.25 μM. The definition of each parameter corresponds to Figure 7B and is explained in the Discussion. The inhibitory effect (α) was calculated as K'/K. The positive cooperativity effect (β) was calculated as A/A'.

The presence of a second alkanol at a concentration near its IC_{50} has the major effect of reducing the initial dissociation constant (A) of the first alkanol. That is, the second alkanol increases the apparent initial affinity of the first alkanol. This effect is much greater with decanol as the second alkanol (330 times) than with octanol (13 times) and reflects the much stronger positive cooperativity effect of decanol. The second alkanol thus makes the first alkanol a stronger inhibitor at low concentrations due to the positive cooperativity effect of the second alkanol. Since the second alkanol is essentially substituting the first alkanol in this action, the second alkanol also decreases the positive cooperativity effect of the first alkanol, resulting in a decreased slope coefficient of the first alkanol. (This decrease was seen in the double-inhibitor experiments whose results are shown in panels B and C of Figure 5, although it was not statistically significant.)

The inhibitory effect (α) of the first alkanol is actually reduced ~2−3-fold by the presence of the second alkanol.

The second alkanol thus makes the first alkanol a weaker inhibitor at high concentrations due to competition with the second alkanol for the second sites. This accounts for the increased fraction of uninhibited binding seen at high concentrations of the first alkanol. The combination of these two counteracting effects results in only a slight decrease in IC_{50} of the first alkanol. This model predicts that the presence of a constant amount of a second alkanol will decrease the slope coefficient of the first alkanol and increase the fraction of uninhibited binding, while having little effect on the IC_{50}. This is what is seen in the results of the double-inhibitor studies shown in panels B and C of Figure 5.

This model is consistent with the reported photolabeling of the desensitized *Torpedo* AChR by 3-azirinyloctanol mainly on α-M2−20′ glutamate residues (*30*), since there are two such residues on each *Torpedo* AChR. In that study, the level of 3-azirinyloctanol labeling was not reduced by octanol near its IC_{50} of 1 mM, which is the expected result if two alkanol sites linked by positive cooperativity are available for binding. Furthermore, photolabeling was not blocked by high concentrations of the cationic NCIs, PCP and QX-222, leading to a proposed structural model where the polar head of the alkanol molecule associates with the top of the α-M2 helix while the tail reaches down into the channel no further than position 15′; in that model, the AChR can simultaneously accommodate a large alkanol molecule and a cationic NCI.

The findings here indicate that the long-chain alkanols do not compete sterically with each other for a single site from which to inhibit [^{3}H]TCP binding to the agonist-desensitized *Torpedo* AChR. These findings, like those of 3-azirinyloctanol photolabeling, are in apparent disagreement with studies on functional AChRs from *Torpedo* (*24*, *26*, *27*) and embryonic mouse muscle (*28*, *29*), which conclude that alkanols inhibit ion flow by binding to a hydrophobic patch in the middle of the M2 channel domain large enough to accommodate only one long-chain alkanol molecule at a time. The most likely explanation of this apparent disagreement is that the alkanol inhibitory site identified on the functional AChR is considerably different from the alkanol site on the desensitized AChR. Several lines of evidence support this explanation. For example, a number of M2 domain-binding NCIs exhibit substantially different affinities for the functional and desensitized AChR conformations (*19*, *51*). In fact, the putative alkanol channel site on the functional *Torpedo* AChR displays a much higher apparent affinity for alkanol than the site(s) producing inhibition of [^{3}H]NCI binding to the desensitized *Torpedo* AChR; for example, *n*-octanol exhibits an IC_{50} of 20−50 μM for the former (*27*) and an IC_{50} of 1−4 mM for the latter (*25*; Table 1). A structural change in the M2 channel domain in the two conformations was clearly demonstrated by the different patterns of M2 segment photolabeling by [^{125}I]-3-(trifluoromethyl)-3-(*m*-iodophenyl)diazirine (TID), a small uncharged NCI (*52*), and by a larger uncharged compound, [^{3}H]diazofluorene (*53*).

Interaction between the Cembranoid and Long-Chain Alkanol Sites. Superficially, the cembranoids resemble the long-chain alkanols and cycloalkanemethanols in being hydrophobic uncharged NCIs of the AChR. In fact, one of the most potent cembranoids, sarcophytol-A (Figure 1), is a large cyclic alcohol. However, unlike hydrophobic alcohols, even the most potent cembranoids do not display an anesthetic effect in vivo when tested in mice and fish (O. R. Pagán et al., unpublished results). The calculated molecular volume of sarcophytol (600 Å^3) is nearly twice the maximum allowable volume estimated for hydrophobic alcohols entering their site on the functional *Torpedo* AChR (*26*). Therefore, it is unlikely that cembranoids bind in the long-chain alkanol site on the functional AChR. However, the above-mentioned difference between the channel domains on the functional and desensitized conformations of the *Torpedo* AChR leaves open the possibility that cembranoids and alkanols could be competing for the same site on the desensitized AChR.

While the findings in this report show that the cembranoid inhibitory site and the alkanol sites on the desensitized *Torpedo* AChR are not independent of each other, the data are inconsistent with simple steric overlap between cembranoid and alkanol sites. The simplest model for cembranoid−alkanol interaction which fits the data shown in Figure 6 is one in which occupancy of both alkanol sites decreases the affinity of cembranoid for its inhibitory site while binding of cembranoid to its inhibitory site decreases the affinity of the second (high-affinity) alkanol site. This model correctly predicts that in the presence of a fixed amount of alkanol the cembranoid inhibition curve will be shifted to the right with minimal change in the slope (Figure 6A,B). On the other hand, in the presence of a fixed amount of cembranoid, the alkanol curve will also be shifted to the right but with an increase in the level of uninhibited [^{3}H]TCP binding (Figure 6C). Therefore, long-chain alkanols and cembranoids interfere with each other for their [^{3}H]TCP inhibitory sites on the desensitized AChR in a manner which is consistent with negative allosteric inhibition. Therefore, the allosteric effect of alkanols on cembranoid binding is similar to the allosteric effect of alkanols on the TCP site, which the cembranoid site overlaps.

The allosteric inhibition of alkanol binding by cembranoids may have potential clinical relevance. While alkanols act centrally as general anesthetics, unpublished studies in this lab have shown no general anesthetic effect on fish or mice by even the most potent cembranoids. If the central anesthetic effect of alkanols, and of other uncharged NCIs, is mediated through a mechanism similar to that which inhibits the peripheral AChR, then cembranoids may be able to reverse this effect without themselves producing anesthesia. This hypothesis can be tested.

In summary, the model for cembranoid binding proposed here provides a structure for experimentally testing how cembranoids interact with the peripheral AChR as well as with neuronal AChRs. This issue is particularly relevant in view of the recent report that both marine and tobacco cembranoids inhibit human neuronal AChRs and can block one of the behavioral effects of nicotine in rats (*35*).

ACKNOWLEDGMENT

We thank Ms. Liz Díaz and Ms. Jessica Soto for their technical assistance, Mr. Amit Misra for his help with the kinetics analysis, and Prof. Karen Grace-Martin (Office of Statistical Consulting, Division of Nutritional Sciences, Cornell University, Ithaca, NY) for her help with the statistical analysis.

REFERENCES

1. Franks, N. P., and Lieb, W. R. (1994) *Nature 367*, 607−614.
2. Evers, A. S., and Steinbach, J. H. (1997) *Anesthesiology 86*, 760−762.
3. Mihić, S. J., Ye, Q., Wick, M. J., Koltchine, V. V., Krasowski, M. D., Finn, S. E., Mascia, M. P., Valenzuela, C. F., Hanson, K. K., Greenblatt, E. P., Harris, R. A., and Harrison, N. L. (1997) *Nature 389*, 385−389.
4. Karlin, A. (1993) *Curr. Opin. Neurobiol. 3*, 299−309.
5. Hucho, F., Tsetlin, V., and Machold, I. (1996) *Eur. J. Biochem. 239*, 539−557.
6. Unwin, N. (1993) *J. Mol. Biol. 229*, 1101−1124.
7. Hucho, F., Oberthur, W., and Lottspeich, F. (1986) *FEBS Lett. 205*, 137−142.
8. Giraudat, J., Dennis, M., Heidmann, T., Haumont, P.-Y., Lederer, F., and Changeux, J.-P. (1987) *Biochemistry 26*, 2410−2418.
9. DiPaola, M., Kao, P. N., and Karlin, A. (1990) *J. Biol. Chem. 265*, 11017−11029.
10. Zhang, H., and Karlin, A. (1997) *Biochemistry 36*, 15856−15864.
11. Bertrand, D., Galzi, J.-L., Devillers-Thiery, A., Bertrand, S., and Changeux, J.-P. (1993) *Curr. Opin. Cell Biol. 5*, 688−693.
12. Blanton, M. P., and Cohen, J. B. (1994) *Biochemistry 33*, 2859−2872.
13. Narayanaswami, V., Kim, J., and McNamee, M. G. (1993) *Biochemistry 32*, 12413−12419.
14. Bouzat, C., and Barrantes, F. J. (1993) *J. Biol. Chem. 271*, 25835−25841.
15. Eterović, V. A., Hann, R. M., Ferchmin, P. A., Rodríguez, A. D., Li, L., Lee, Y. H., and McNamee, M. G. (1993) *Cell. Mol. Neurobiol. 13*, 99−110.
16. White, B. H., Howard, S., Cohen, S. G., and Cohen, J. B. (1991) *J. Biol. Chem. 266*, 21595−21607.
17. Gage, P. W., McBurney, R. N., and Schneider, G. T. (1975) *J. Physiol. 244*, 409−429.
18. Dilger, J. P., and Vidal, A. M. (1994) *Mol. Pharmacol. 46*, 169−175.
19. Arias, H. R. (1996) *Mol. Membr. Biol. 13*, 1−17.
20. Heidmann, T., Oswald, R. E., and Changeux, J.-P. (1983) *Biochemistry 22*, 3112−3127.
21. Changeaux, J.-P. (1981) *Harvey Lect. 75*, 85−254.
22. Niu, L., and Hess, G. P. (1993) *Biochemistry 32*, 3831−3835.
23. Bradley, R. J., Sterz, R., and Peper, K. (1984) *Brain Res. 295*, 101−112.
24. Wood, S. C., Forman, S. A., and Miller, K. W. (1991) *Mol. Pharmacol. 39*, 332−338.
25. El-Fakahany, E. F., Miller, E. R., Abbassy, M. A., Eldefrawi, A. T., and Eldefrawi, M. E. (1983) *J. Pharmacol. Exp. Ther. 224*, 289−296.
26. Wood, S. C., Hill, W. A., and Miller, K. W. (1993) *Mol. Pharmacol. 44*, 1219−1226.
27. Wood, S. C., Tonner, P. H., Armendi, A. J., Bugge, B., and Miller, K. W. (1995) *Mol. Pharmacol. 47*, 121−130.
28. Forman, S. A., Miller, K. W., and Yellen, G. (1995) *Mol. Pharmacol. 48*, 574−581.
29. Zhou, Q. L., Zhou, Q., and Forman, S. A. (2000) *Biochemistry 39*, 14920.
30. Pratt, M. P., Husain, S. S., Miller, K. W., and Cohen, J. B. (2000) *J. Biol. Chem. 275*, 29441−29451.
31. Rodriguez, A. D. (1995) *Tetrahedron 51*, 4571−4618.
32. Ciereszko, L. S. (1991) *Biological Oceanography 6*, 363−374.
33. Coll, J. C., Bowden, B. F., Tapiolas, D. M., and Dunlap, W. C. (1982) *J. Exp. Mar. Biol. Ecol. 60*, 293−299.
34. Wahlberg, I., and Eklund, A.-M. (1992) in *Progress in the chemistry of organic natural products* (Herz, W., Kirby, G. W., Moore, R. E., Steglich, W., and Tamm, C., Eds.) Vol. 59, pp 142−294, Springer-Verlag, New York.
35. Ferchmin, P. A., Lukas, R. J., Hann, R. M., Fryer, J. D., Eaton, J. B., Pagán, O. R., Rodríguez, A. D., Nicolau, Y., Rosado, M., Cortés, S., and Eterović, V. A. (2001) *J. Neurosci. Res. 64*, 18−25.
36. Abramson, S. N., Li, Y., Culver, P., and Taylor, P. (1989) *J. Biol. Chem. 264*, 12666−12672.
37. Hann, R. M., Pagán, O. R., Gregory, L. M., Jácome, T., Rodríguez, A. D., Ferchmin, P. A., Lu, R. and Eterović, V. A. (1998) *J. Pharmacol. Exp. Ther. 287*, 253−260.
38. Pagán, O. R. (1998) M.S. Thesis, University of Puerto Rico Medical Sciences Campus, San Juan, PR.
39. Szczawinska, K., Ferchmin, P. A., Hann, R. M., and Eterović, V. A. (1992) *Cell. Mol. Neurobiol. 12*, 95−106.
40. Lowry, O. H., Roseborough, N. J., Farr, A. L., and Randall, J. R. (1951) *J. Biol. Chem. 193*, 265−275.
41. Schmidt, J., and Raftery, M. A. (1973) *Anal. Biochem. 52*, 349−354.
42. Song, X.-Z., and Pedersen, S. E. (2000) *Biophys. J. 78*, 1324−1334.
43. Lin, L., Koblin, D. D., and Wang, H. H. (1995) *Biochem. Pharmacol. 49*, 1085−1089.
44. Kostenis, E., and Mohr, K. (1996) *Trends Pharmacol. Sci. 17*, 280−283.
45. Lurtz, M. M., Hareland, M. L., and Pedersen, S. E. (1997) *Biochemistry 36*, 2068−2075.
46. Pratt, M. P., Pedersen, S. E., and Cohen, J. B. (2000) *Biochemistry 39*, 11452−11462.
47. Mosckovitz, R., Haring, R., Gershoni, J. M., Kloog, Y., and Sokolovsky, M. (1987) *Biochem. Biophys. Res. Commun. 145*, 810−816.
48. Blanton, M. P., McCardy, E., and Gallagher, M. J. (2000) *J. Biol. Chem. 275*, 3469−3478.
49. Katz, E. J., Cortes, V. I., Eldefrawi, M. E., and Eldefrawi, A. T. (1997) *Toxicol. Appl. Pharmacol. 146*, 227−236.
50. Gallagher, M. J., and Cohen, J. P. (1999) *Mol. Pharmacol. 56*, 300−307.
51. Blanchard, S. G., Elliot, J., and Raftery, M. A. (1979) *Biochemistry 18*, 5880−5884.
52. White, B. H., and Cohen, J. B. (1992) *J. Biol. Chem. 267*, 15770−15783.
53. Blanton, M. P., Dangott, L. J., Raja, S. K., Lala, A. K., and Cohen, J. B. (1998) *J. Biol. Chem. 273*, 8659−8668.

BI0112255